Transient Plumes from Convective Flow Instability in Horizontal Cylinders

Foluso Ladeinde* and K. E. Torrance†
Cornell University, Ithaca, New York 14853

In this paper we report on a transient flow instability phenomenon in a horizontal cylinder whose wall is subjected to a step increase in temperature. Pertinent previous work on related subjects is reviewed, and the appropriate governing equations and their numerical simulation are discussed for the present problem. The flow is governed by the Rayleigh number Ra as the other parameters are kept fixed. Studies are carried out for $0 \leq Ra \leq 10^6$. The flowfield consists of two cells for $Ra \leq 10^5$. Boundary layers at the wall exhibit a filling box phenomenon, which leads to a vertical stable stratification of the interior temperature field. The two-cell mode is temporarily unstable at $Ra = 10^6$, and a plume from a point source of buoyancy at the bottom of the cylinder evolves early in the transient. The downward motion of the stratification front suppresses the growth of the plume, and the flow is restabilized as the front approaches the bottom of the cylinder. The initial and final state in the system is a motionless fluid isothermal at the initial and new wall temperatures, respectively.

Nomenclature

e_a	= unit vector in the direction indicated by a
g	= gravity vector, m/s²
g	= absolute value of the gravity vector, m/s²
k	= thermal conductivity, W/m · K
O	= origin of the inertial coordinate frame
P	= dimensional total pressure, N/m²
Pr	= Prandtl number
p	= dimensionless reduced pressure
R	= radius of cylinder, m
Ra	= gravitational Rayleigh number
r	= radial direction in polar coordinate
t	= dimensionless time
T	= dimensionless temperature
T_b	= bulk temperature
T_m	= volume-averaged temperature
t	= dimensionless time
u	= dimensionless velocity in X or x direction
u_r	= dimensionless velocity in r direction
u_θ	= dimensionless velocity in θ direction
u	= $(u,v)^*$, $(u,v,w)^*$ or $(u,v,T)^*$ depending on context
v	= dimensionless velocity in Y or y direction
w	= dimensionless velocity in Z or z direction
X,x	= x direction in inertial Cartesian frame of reference
Y,y	= y direction in inertial Cartesian frame of reference
Z,z	= z direction in inertial Cartesian frame of reference
α	= thermal diffusivity, m²/s
β	= thermal expansion coefficient, 1/K
ΔT	= temperature difference $T - T_o$, K
$\Delta \bar{T}$	= temperature difference $T_w - T_o$, K
Δt	= time step size
ζ	= axial vorticity

θ	= azimuthal direction in polar coordinate
ν	= kinematic viscosity, m²/s
π	= viscosity ratio
ρ	= dimensional fluid density, kg/m³
ψ	= Stokes stream function

Subscripts

o	= reference value, hydrostatic
w	= wall

Superscript

*	= transpose

Introduction

THE present study pertains to gravity-driven thermal convection in a horizontal cylinder. The need for a more detailed understanding of the system has been motivated by the wide industrial application. Such applications include the use as heating vessels in chemical industries, extended solar heating of chemical (e.g., petroleum) storage vessels on hot days (with particular relevance to the tropics), cooling of containers for storing heat-producing fluids, and the cooling of liquid hydrogen and liquid deuterium moderators and targets for high-energy physics experiments. Crystal growth ampoules (e.g., in the preparation of semiconductors, insulators, and metals, in materials processing) are long horizontal cylinders which are subjected to substantial axial temperature gradients by the furnaces in which they are placed. The latter application might involve microgravity and an inclination of the residual gravity vector. Other important applications of the present work are the transient heating of horizontal oil pipelines for the restart (refluidization) of the oil flow and the transient cooling of pipes and containers filled with water and their eventual freezing in cold climates. Studies of thermal convection in a horizontal cylinder are also of intrinsic academic interest.

Previous studies on horizontal cylinders can be grouped according to how the motion is generated vis-a-vis the imposed temperature gradient. These groups include the imposition of a temperature gradient on the bounding surface,[1,2] a uniform and constant heat flux on the surface,[3] a volumetric heat generation,[4] and keeping the wall at a uniform temperature that changes with time at a constant rate.[5] In other studies[6] and the present one, flow is driven by a step-change in wall temperature.

*Graduate Research Assistant, Sibley School of Mechanical and Aerospace Engineering; currently fluid/aerodynamist at Technalysis Inc., Indianapolis, IN. Member AIAA.

†Professor, Sibley School of Mechanical and Aerospace Engineering.

The flows in these systems usually consist of two-cell convection modes at low to moderate parameter values, except in the system in which flows are driven by a specified temperature gradient at the wall. The possible mode for this latter case ranges from a single-cell pattern to a multicellular pattern, depending on the manner (wall-region) in which the temperature gradient is imposed.

The experimental investigations by Maahs and David,[3] Deaver and Eckert,[5] and Beloff et al.[7] have shown that the two-cell mode is unstable at higher parameter values, and other convective modes have sufficient amplitudes to modify the flowfield. Depending on whether the surface is heated or cooled, eddies are formed at the bottom (top) of the cylinder. The instability is manifested in what we refer to as thermal plumes in the temperature field. (See Townsend[8] for the appropriateness of the terminology "thermal plume.") Except for the interferometric studies by Hauf and Grigull[6] only very sketchy details have been given for the instability phenomenon. The localized eddies are usually represented by hand sketches, and the plume structure in the temperature field is never reported. The flow was not visualized in the study by Hauf and Grigull. Also, we are not aware of any numerical or analytical studies that have reported on the instability.

There are several features of the present problem that could pose considerable difficulties for most numerical methods. First, the instability starts out as weak eddies. We believe that dissipative time integration schemes would "wash off" the weak eddies unless the time step size is sufficiently small at the time the eddies are being formed. (This latter requirement is independent of any numerical stability restriction on time step size.)

The second factor is related to the singularity at the axis of the cylinder. The singularity poses considerable difficulties for the finite difference method for transient Navier-Stokes.[9] The errors introduced by ad hoc numerical techniques for handling the singularity are expected to be very serious at the large amplitude of the flows in the plume regime. Third, the transient nature of the present problem is such that large amplitude flows occur only for a relatively small fraction of the total transient period. Therefore, time integration schemes in which the time step size is chosen with due regards for the physics (not necessarily the numerical stability) of the flow are very useful. Also, we should be able to set a maximum limit on the time integration error allowed at any time step.

The finite difference calculations by Takeuchi and Cheng[10] probably contacted one of the first two problems above. Their study was a numerical investigation of the problem studied experimentally by Deaver and Eckert. However, while the bottom eddies were observed at Rayleigh number (to be defined later) of $Ra = 6 \times 10^6$ in the experiments, the finite difference calculations did not pickup the eddies even at $Ra = 10^7$. Takeuchi and Cheng ascribed the discrepancy to the relatively early termination of the calculations.

We have developed a penalty Galerkin finite element code[11] with capabilities to handle the foregoing difficulties. The purpose of the present paper is to report on a successful simulation of the instability phenomenon with the code. We also want to discuss the heat-up processes and the physics of flow in the system for a fairly wide range of parameter values.

In the next section, we will give the Boussinesq equations governing thermal convection in a horizontal cylinder, and the parameters of the problem will be identified. This is followed by a brief description of the various schemes for temporal and spatial integration of the governing equations. Thereafter, results are discussed for a range of parameter values, which include the plume regime. Concluding remarks and a list of references are given at the end of the paper.

Governing Equations

The physical model and coordinates are shown in Fig. 1a. The equations for thermal convection in an incompressible
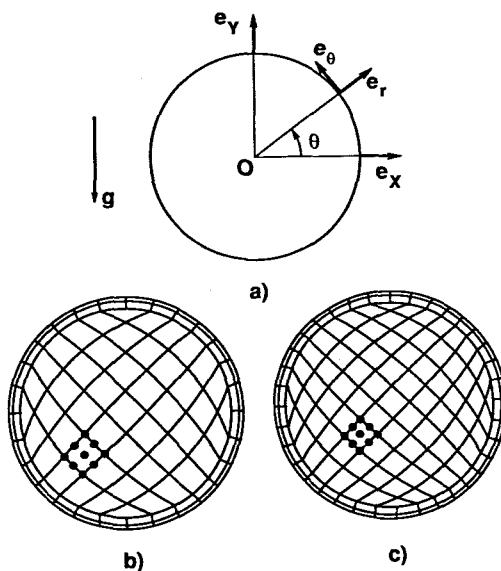

Fig. 1   Physical model and computation grid.

viscous fluid are those stating the conservation of mass, momentum, and energy. The appropriate Boussinesq equations for the present problem are

$$\nabla \cdot u = 0 \tag{1}$$

$$\frac{\partial u}{\partial t} + u \cdot \nabla u = -\nabla p + Pr \nabla \cdot \pi$$

$$[\nabla u + (\nabla u)^*] + RaPrTB \tag{2}$$

$$\frac{\partial T}{\partial t} + u \cdot \nabla T = \nabla^2 T \tag{3}$$

where

$$u = (u,v,w)^*, \qquad B = (0,1,0)^*$$

$$Pr = \nu_0/\alpha = \text{Prandtl number}$$

and

$$Ra = \frac{g\beta \overline{\Delta T} R^3}{\nu \alpha} = \text{gravitational Rayleigh number}$$

Also, the nondimensional viscosity, π, which requires a specifying equation appears. A superscripted asterisk on brackets implies the transpose of the tensors in the brackets. The properties involved include ν, α, g, β, R, which are the kinematic viscosity of the fluid (with a reference value of ν_0), the thermal diffusivity of the fluid, the absolute value of the normal gravity vector, the thermal expansion coefficient, and the radius of the cylinder. The pressure p that appears in Eq. (2) is the reduced pressure

$$p = \frac{R^2}{\rho_0 \alpha^2} [P + \rho_0 g y]$$

and $\overline{\Delta T} = T_w - T_0$

We have restricted the present calculation to a two-dimensional domain in the (r,θ) coordinates of the cylinder in order to avoid the large computer time and memory needed for time-dependent, three-dimensional simulations. Moreover, no significant motion in the axial direction has been reported for the flows in the instability regime. All the flows studied in the present paper are laminar.

The initial condition in the system is

$$u = 0, \; T = 0$$

u and T are finite at $r = 0$

and the conditions on the surface of the cylinder are

$$u = 0, \text{ and } T = 1 \; (r = 1)$$

The Stokes stream function ψ and the axial component of vorticity ζ can be obtained from the relation

$$\zeta = \frac{1}{r}\frac{\partial}{\partial r}(ru_\theta) - \frac{1}{r}\frac{\partial u_r}{\partial \theta} = -\Delta\psi \qquad (4)$$

where

$$\Delta \equiv \frac{\partial^2}{\partial r^2} + \frac{1}{r}\frac{\partial}{\partial r} + \frac{1}{r^2}\frac{\partial^2}{\partial \theta^2}$$

The heat-up process in the system can be described by the variation with time of some "average" temperature. Two quantities, T_m and T_b, have been used for this purpose. We have defined them as follows:

$$T_m = \frac{\displaystyle\int_0^1\int_0^{2\pi} Tr \, d\theta \, dr}{\displaystyle\int_0^1\int_0^{2\pi} r \, d\theta \, dr}$$

and

$$2T_b = \frac{\displaystyle\int_{-1}^{1} u(x_1^*)T(x_1^*) \, dy}{\displaystyle\int_{-1}^{1} u(x_1^*) \, dy} + \frac{\displaystyle\int_{-1}^{1} v(x_2^*)T(x_2^*) \, dx}{\displaystyle\int_{-2}^{1} v(x_1^*) \, dx}$$

where x_1^* and x_2^* denote the vertical diameter and the horizontal diameter, respectively. Thus T_m is the volume-averaged temperature, and T_b is the average of the two temperatures obtained by collecting and mixing together fluids crossing the vertical diameter and those crossing the horizontal diameter. Better results are expected for T_b when more diameters than two are used for the calculation.

Finite Element Solution

A brief discussion of the numerical schemes used in the computer code is provided in this section. The code is based on the consistent (not the reduced integration) penalty Galerkin finite element method. It uses a predictor-corrector scheme, with or without a time integration error control. It also uses
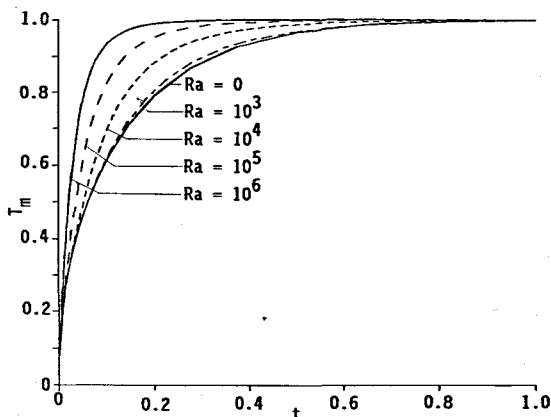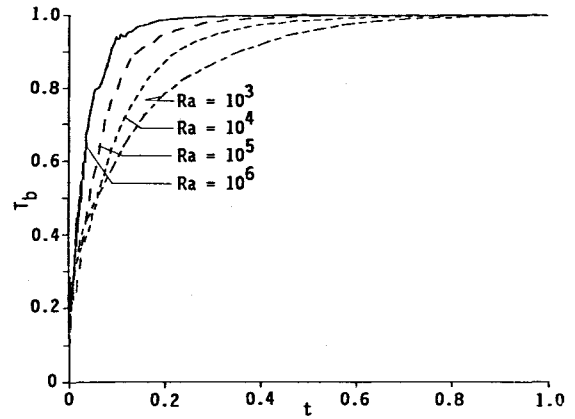

Fig. 3   Transient bulk temperature.

one of the best known elements for Navier-Stokes (i.e., biquadratic continuous Lagrange interpolation for velocities and temperature and a linear discontinuous interpolation for pressure). The code allows a constant time step size integration, or the physics of the flow could be followed to choose the appropriate time step size which ensures a preset condition on the maximum (local) time integration error. Both time integration schemes could also be combined in one simulation. We believe that comparable capability to those discussed above are needed for a successful and cost-effective simulation of the instability phenomenon. The Newton-Raphson procedure has been implemented for linearizing the convective terms of the momentum and energy equations, and the assembled equations are solved using the skyline method. The mathematical details of the various schemes are not given in this paper. Interested readers could consult Ladeinde[11] for details.

Results and Discussions

In this section we will describe the observed flow and temperature fields in our numerical simulation of normal gravity-driven thermal convection in a horizontal cylinder for Ra values up to 10^6. The initial and final state for this problem is a motionless fluid isothermal at the initial and the new wall temperatures, respectively. Thus, the motion occurs between the two stagnant states.

The code used for the present problem has undergone very stringent tests to establish its validity. Such tests include isothermal and nonisothermal, free and forced, transient and steady flows, with or without volumetric heat generation. The code has also been tested for convection in rotating and self-gravitating cylinders rotating about their axes in a normal gravity field. However, no purpose is served by a further discussion on the test cases.

We have provided Figs. 1–16 for the discussions of the results obtained in the present study. Figures 1b and 1c show the computational grids used for the calculations. Figure 1b, which consists of 105 element and 449 nodes, was used for the simulations involving $Ra \leq 10^5$. Figure 1c has 153 elements and 649 nodes and was used for the simulations involving $Ra = 10^6$. The heat-up process in the system is presented in Figs. 2 and 3 in terms of the volume-averaged temperature and the bulk temperature. A convective instability phenomenon observed at early time in flows involving $Ra = 10^6$ will be discussed later in this paper. One manifestation of the phenomenon is the large amplitude associated with the oscillation about zero of the stream function values at cavity center. From Fig. 3 we observe that the latter process is also manifested in the bulk temperature profile. Such oscillations are absent in the volume-averaged temperature. Therefore the bulk temperature concept introduced in this paper is probably a more accurate measure of heat up in the system than the
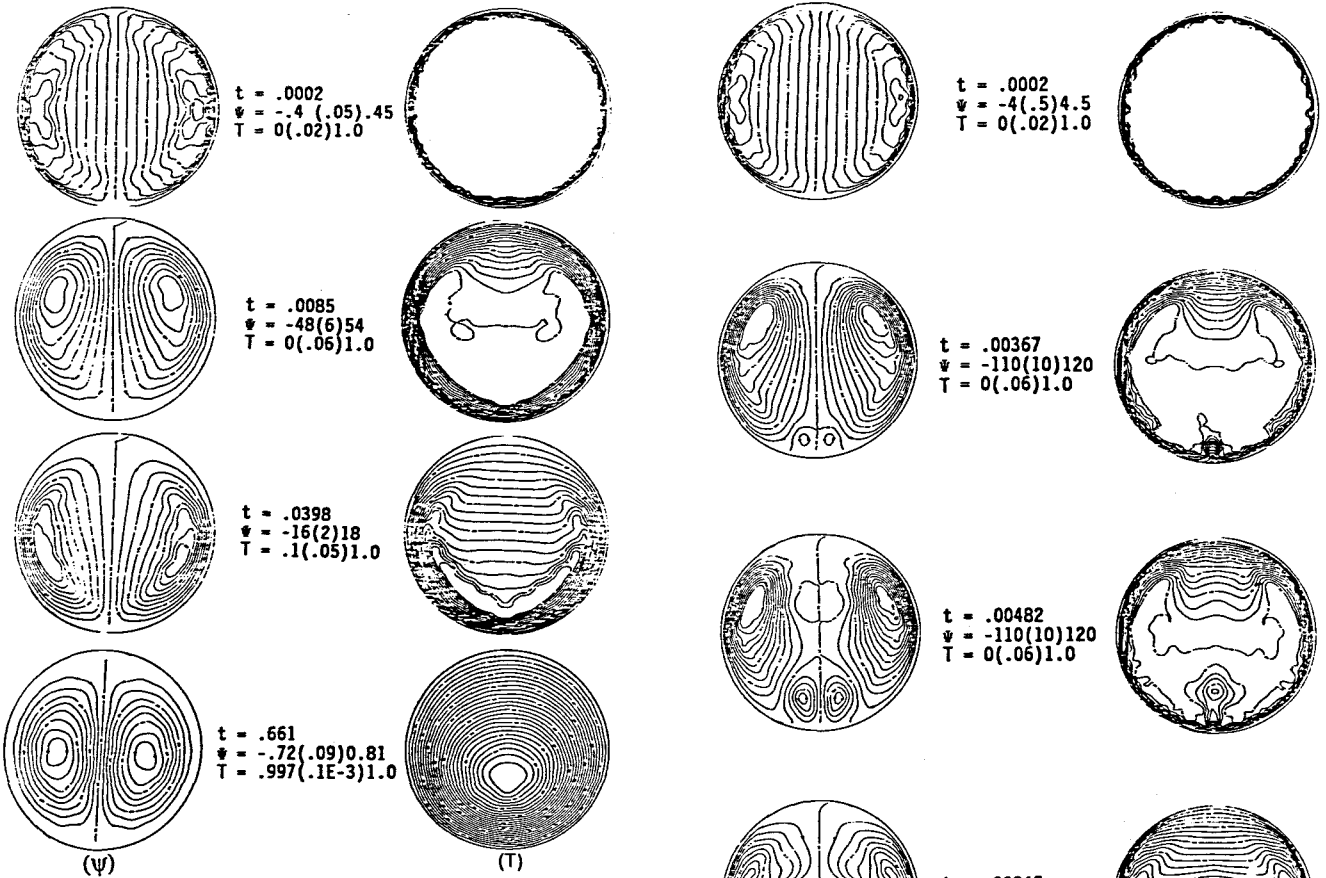

Fig. 2   Transient volume-averaged temperature.

Fig. 4   Transient motion at $Ra = 10^5$ (note that $T_w = 1$, $\psi_w = 0$).

volume-averaged temperature, especially if more diameters than two are used for calculating the bulk temperature.

The transient flowfields show similar qualitative behavior for all nonzero Ra values up to 10^5, and the typical case of $Ra = 10^5$ is used for the discussions. The flowfields for $Ra = 10^6$ are also discussed since these are quite different from those for lower Ra values studied.

The temporal development of the flowfield is rather simple for $Ra \leq 10^5$ and consists of an initially weak two-cell pattern (kidney beans) that relaxes into "fuller" cells as the flow approaches the final state (see Fig. 4). The two-cell circulation pattern in meridian (r, θ in this problem) plane is a familiar one from previous experimental studies and from the finite difference study by Takeuchi and Cheung. The convection cells are due to the gravitational torque [i.e., $g \times \nabla\rho$, where $\rho = \rho_0 (1 + \beta\Delta T)$], the associated vorticity vector being axial in direction. Since gravity is directed vertically downwards, and the wall of the cylinder is heated, lighter, high temperature fluid at the wall is transported upwards and, by mass conservation, is replaced by cooler fluid from the interior. The process is continued as the latter fluid is in turn heated and transported to the interior.

A filling box phenomenon[12] that results from the laminar convection boundary layers at the "vertical" wall is noticeable in the temperature field at $t = 0.0085$ and has become evident at $t = 0.0398$. The consequent stable vertical stratification of the temperature field can be observed at this time from the isotherms. (Note the downward movement with time of the stratification front.) The flow increases in strength (as measured by stream function) from an initial value of 0 to a peak value of approximately 50 at $t = 0.0085$. The flow decreases in strength thereafter and has become quite weak by $t = 0.6610$. An isothermal condition has essentially been established in the cylinder at this time (temperature is approximately unity at all
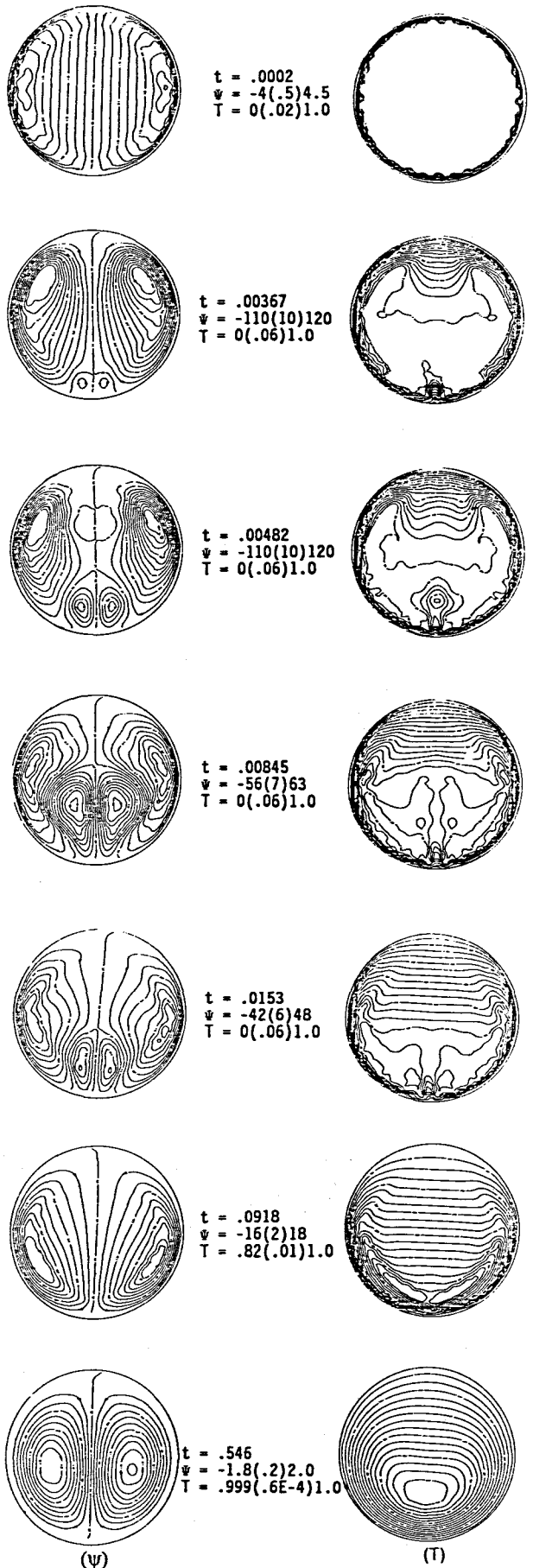
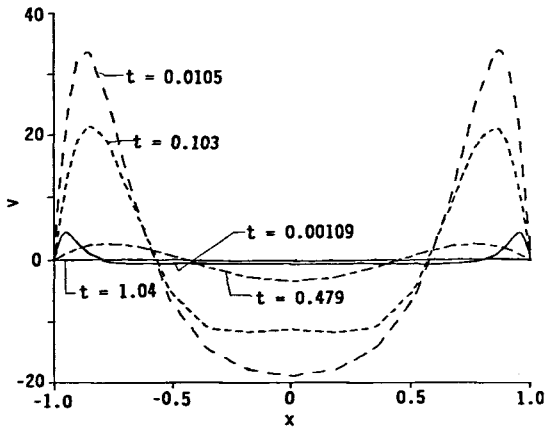**Fig. 5   Transient motion at $Ra = 10^6$ (note that $T_w = 1$, $\psi_w = 0$).**

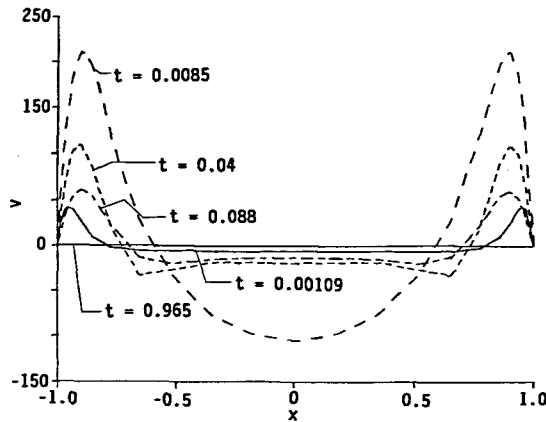Fig. 6 Vertical velocity component along the horizontal diameter ($Ra = 10^4$).

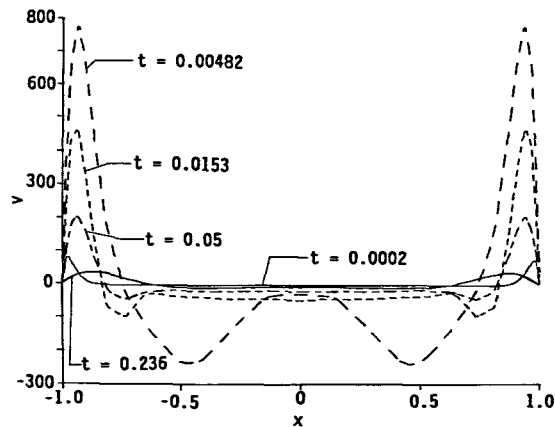Fig. 7 Vertical velocity component along the horizontal diameter ($Ra = 10^5$).

Fig. 8 Vertical velocity component along the horizontal diameter ($Ra = 10^6$).

hot fluid in the form of eddies has risen above the heated wall by $t = 0.00367$ and more fluid is subsequently drawn in (entrained) and heated. Momentum flux presumably increases with distance up the plume through the action of normal gravitational buoyancy. The mass flux also increases as the plume entrains neighboring fluids. The entrainment process results in a continuous growth of the eddy region, and the two main convection cells are continuously pushed towards the wall by the growth of the eddies because of the weaker flows
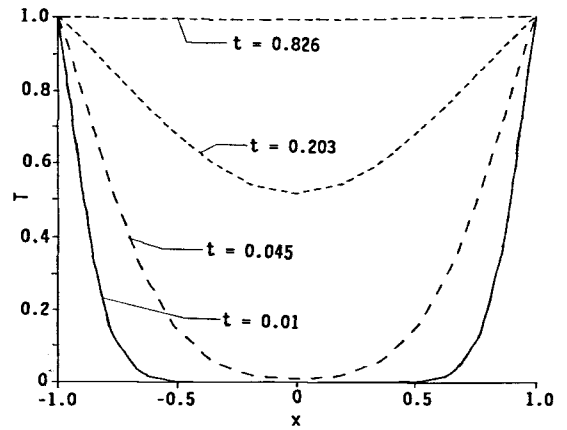

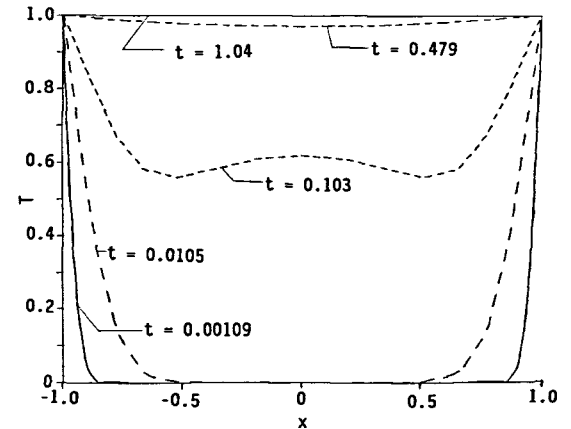Fig. 9 Conduction temperature profile along the horizontal diameter.

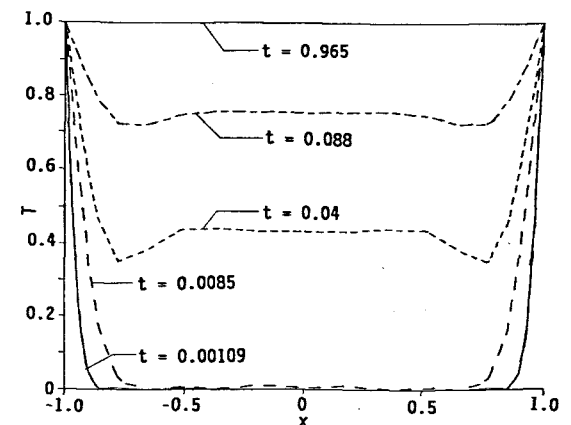Fig. 10 Temperature distribution along the horizontal diameter ($Ra = 10^4$).

Fig. 11 Temperature distribution along the horizontal diameter ($Ra = 10^5$).

points in the cylinder). Fluid viscosity ultimately damps out the residual velocities.

The flowfield observed at $Ra = 10^6$ (see Fig. 5) is distinguished by the large strength and the production of a laminar thermal plume that originates from a point source of buoyancy in the bottom region of the heated wall. (Note that the gravitational potential energy is greatest at the bottom of the cylinder, and the bottom therefore represents a point source of buoyancy relative to neighboring points.) A weak column of

in the outer part of the main cells. A substantial growth of the eddies is observed only after the maximum flow strength has occurred. We observe from the figures that the eddy region (and the associated plume) subsequently gets smaller, finally disappearing as the flow approaches zero strength. We also note that a portion of the fluid has not felt the heat input at the wall, and the minimum temperature is still zero by the time the eddy region starts to disappear. The latter observation is presumably due to the value of the Prandtl number used ($Pr = 7$). We also believe that a finer grid than 649 mesh points is needed for a more accurate solution at short time. Nevertheless, the performance of this coarse grid is rather impressive for this complicated problem. Qualitative support for the flow documented in this paper is provided by the experimental studies of Hauf and Grigull[6] and the recent investigation of Beloff et al.[7]

Concerning the disappearance of the plume we note that the continuous downward movement of the stratification front suppresses the growth of the instability at the bottom region, as the instability (presumably) does not have sufficient inertia to penetrate the stratified region. The flow is restabilized when the front approaches the bottom of the cylinder.

It is pointed out that the flowfield in the instability flow regime is laminar despite the complicated flow and temperature fields observed. This conclusion is reached on account of the rather coarse mesh used in the present calculations. Deaver and Eckert have also suggested a laminar flow for the instability regime.

Figures 6–8 show the distribution of the vertical component of velocity along the horizontal diameter for $Ra = 10^4$, 10^5,

and 10^6. In general there is an upward flow at the sidewalls and a much weaker downward flow in the interior. The high velocity region gets more and more confined to the sidewalls as the viscous boundary layers become more prominent at larger parameter values. Isotherms for conduction ($Ra = 0$) are concentric circles with center at the origin. The conduction temperature profile along the horizontal diameter is shown in Fig. 9. With increasing Ra thermal boundary layers result in a temperature distribution (along the horizontal diameter) in which high temperature gradients are increasingly confined to the sidewalls, with uniform values of temperature in the interior (Figs. 10–12). The horizontal component of velocity across the vertical diameter is in general much weaker than the upward flow. The magnitude of such flows is insignificant for $Ra \le 10^5$. At $Ra = 10^6$, a relatively strong horizontal flow is observed across the vertical diameter, although such flows are confined to the eddy region at the bottom half of the cylinder (see Fig. 13). Concerning the temperature distribution along the vertical diameter, we observe that the parabolic (conduction) profile about $y = 0$ becomes more and more skewed towards $y = -1$ with increasing Ra so that an increasingly higher temperature gradient is produced at the bottom of the cylinder (Figs. 14 and 15). The instability in the bottom half of the cylinder is attributable to the high heat flux in that region.

The relatively large amplitude of the oscillation (in the stream function at the center) for simulations involving $Ra = 10^6$ is shown in Fig. 16. The behavior is not an artifact introduced by the numerical procedure, and it is expected from the physics of the flow. Studies devoted to such behaviors are available in Staehle and Hahne[13] (and the references
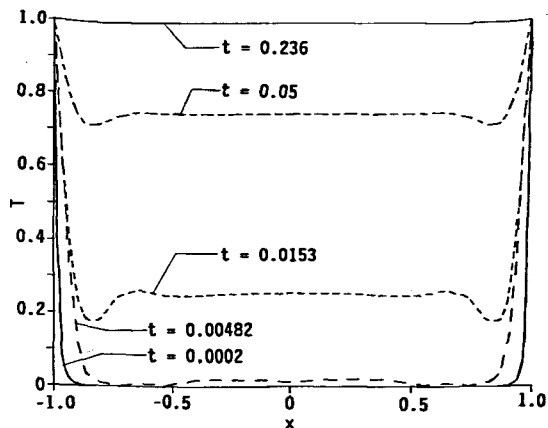

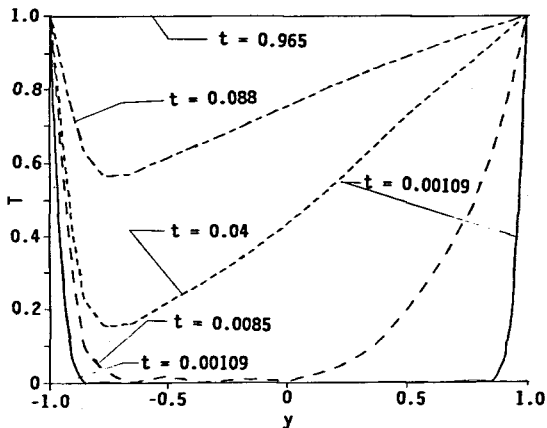Fig. 12　Temperature distribution along the horizontal diameter ($Ra = 10^6$).

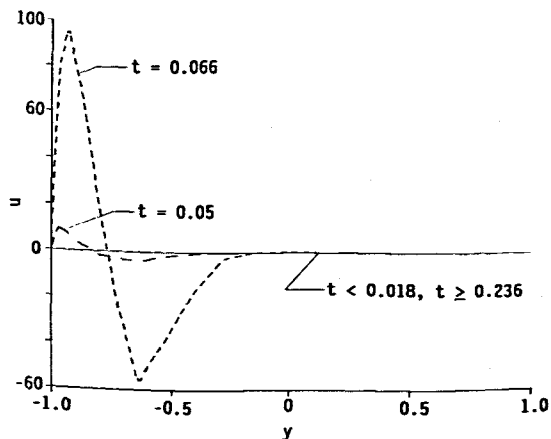Fig. 14　Temperature distribution along the horizontal diameter ($Ra = 10^5$).

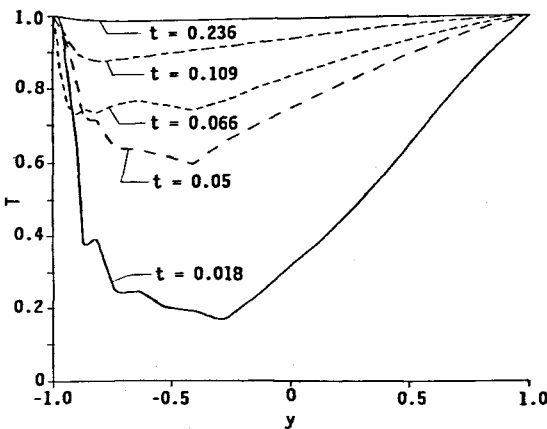Fig. 13　Temperature distribution along the horizontal diameter ($Ra = 10^6$).

Fig. 15　Temperature distribution along the horizontal diameter ($Ra = 10^6$).
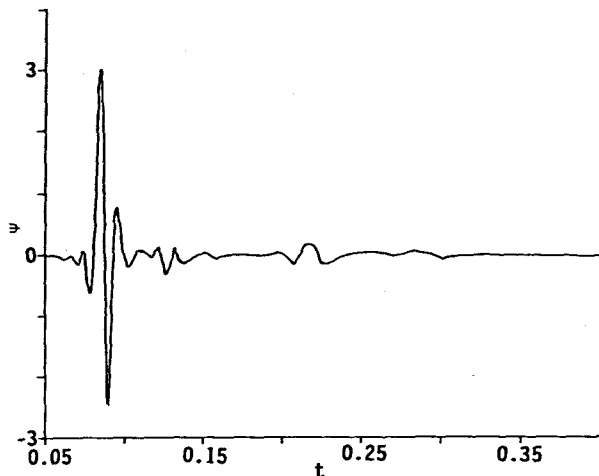
Fig. 16 Variation of cavity center stream function with heating time ($Ra = 10^6$).

therein). Based on our experience, we believe that, although the grid used is not fine enough to give highly accurate results, it is sufficiently fine not to cause the (apparently) random temporal behavior alluded to above. Also, such behaviors could not possibly have resulted from inappropriately large time step size because of the control of the maximum time integration error in our code ($\leq 0.2\%$). The amplitude of such oscillations (or the implied low damping factor) are negligible at lower Ra values with amplitudes of $O(10^{-6})$ for $Ra = 10^5$. The behavior is also dependent on the Prandtl number and on geometric factors.[13]

The studies on the onset of similar behaviors (random effects) in convection layers and the subsequent time-dependence (or transition to turbulence) of the flow have been reviewed by Busse.[14] The critical Ra for the onset of the oscillations (instability) is clearly within the range $10^5 < Ra \leq 10^6$ for the present problem, but it is clear that the potential (temporal) dynamics of the resulting flow cannot be realized because of the transient nature of the present problem.

Conclusion

In this paper we presented the result of a Galerkin finite element simulation of the transient flows between two stagnant states in a horizontal cylinder. The flow is governed by the Rayleigh number, the Prandtl number, and the viscosity ratio. Studies were carried out for Ra values up to 10^6, and the Prandtl number and the viscosity ratio were kept fixed at 7 and 1, respectively.

For $Ra \leq 10^5$, the flowfield consists of two cells. Bifurcations from the two-cell mode originated from the bottom of the cylinder at $Ra = 10^6$. The instability is manifested as a thermal plume in the temperature field.

We believe that a successful numerical simulation of the instability phenomenon requires a nondissipative time integration scheme so as not to damp out the rather weak eddies that are formed at the beginning (in an Ra and/or time space) of the instability. An error control scheme that follows the physics of the flow is recommended if the physics of the flow is of interest, and schemes that avoid ad hoc techniques for handling the singularity at the cylinder axis might be mandatory. An accurate code for the present problem would be one that picks up the bottom eddies as soon (in and Ra and/or time space) as the eddies are formed. The gravitational potential energy is very large at higher Ra, and the eddies are very strong and not easily dissipated numerically. The limiting processes are expected to resemble heating the cylinder from the bottom half and cooling it from the top half. Bottom eddies are the expected main convection mode in this case, as

this limit represents the cylinder "analog" of the Bénard problem. (Only a quasisteady state may be possible in this limit.) The latter flows have been simulated in a steady-state finite difference calculation[15] and in a small amplitude finite difference calculation.[16] Gershuni and Zhukhovitskii[7] have examined the small amplitude instability of the equilibrium of fluid within a horizontal cylinder heated from below using variational mathematics.

References

[1]Ostrach, S., "Natural Convection in Enclosures," *Advances in Heat Transfer*, Vol. 8, 1972, pp. 162–227.

[2]Bontoux, P., Smutek, C., Roux, B., and Lacroix, J. M., "Three-dimensional Buoyancy-Driven Flows in Cylindrical Cavities with Differentially Heated Endwalls," *Journal of Fluid Mechanics*, Vol. 169, 1986, pp. 211–227.

[3]Maahs, H. G., and David, M. M., "Transient Natural Convection Heat Transfer in a Horizontal Cylinder," *The Trends in Engineering*, Vol. 20, No. 7, 1968, pp. 8–20.

[4]Van Sant, J. H., "Free Convection of Heat-Generating Liquids in a Horizontal Pipe," *Nuclear Engineering and Design*, Vol. 10, 1969, pp. 349–355.

[5]Deaver, F. K., and Eckert, E. R. G., "An Interferometric Investigation of Convective Heat Transfer in a Horizontal Fluid Cylinder with Wall Temperature Increasing at a Uniform Rate," *Fourth International Heat Transfer Conference*, Vol. IV, Elsevier, Amsterdam, 1970, pp. NC1.1(1)–NC1.1(12).

[6]Hauf, W., and Grigull, U., "Instationarer Warmeubergang Durch Freje Kenvoktion in Horizontalen Zylindrischen Behaltein," *Fourth International Heat Transfer Conference*, Paris-Versailles, Vol. IV, 1970, pp. NC(1)–NC1(12).

[7]Beloff, P. S., Bejan, A., and Campo, A., "Transient Natural Convection Heat Transfer in a Large-Diameter Cylinder," *Experimental Thermal and Fluid Science*, Vol. 1, 1988, pp. 267–274.

[8]Townsend, A. A., "Turbulent Convection of Heat and Passive Contaminants," *The Structure of Turbulent Shear Flow*, 2nd ed., Cambridge University, Cambridge, UK, 1980, p. 367.

[9]Kee, R. J., and McKillup, A. A., "A Numerical Method for Predicting Natural Convection in Horizontal Cylinders with Asymmetric Boundary Conditions," *Computers and Fluids*, Vol. 5, 1977, pp. 1–14.

[10]Takeuchi, M., and Cheng, K. C., "Transient Natural Convection in Horizontal Cylinders with Constant Cooling Rate," *Warme-und Stoffubertragung*, Vol. 9, 1976, pp. 215–225.

[11]Ladeinde, F., "Studies on Thermal Convection in Self-Gravitating and Rotating Horizontal Cylinders in a Vertical External Gravity Field," Ph.D. Thesis, Sibley School of Mechanical and Aerospace Engineering, Cornell Univ., Ithaca, NY, 1988, pp. 1–346.

[12]Worster, M. G., and Leitch, A. M., "Laminar Free Convection in Confined Regions," *Journal of Fluid Mechanics*, Vol. 156, 1985, pp. 301–319.

[13]Staehle, B., and Hahne, E., "Overshooting and Damped Oscillations of Transient Natural Convection Flows in Cavities," *Heat Transfer*, Paper NC28, Hemisphere, New York, 1982, pp. 287–292.

[14]Busse, F. H., "Transition to Turbulence in Rayleigh-Bénard Convection," *Hydrodynamics Instabilities and the Transition to Turbulence*, edited by H. L. Swiney and J. P. Gollub, Springer-Verlag, Berlin, 1981, pp. 97–137.

[15]Patankar, S. V., Ramadhyani, S., and Sparrow, E. M., "Effect of Circumferentially Nonuniform Heating on Laminar Combined Convection in a Horizontal Tube," *Journal of Heat Transfer*, Vol. 100, 1978, pp. 63–70.

[16] Leong, S. S., and de Vahl Davis, G., "Natural Convection in a Horizontal Cylinder," International Conference on Numerical Methods in Thermal Problems, Swansea, UK, Rept. 1979/FMT/5.

[17]Gershuni, G. Z., and Zhukhovitskii, E. M., "The Stability of Equilibrium of Fluid Within a Horizontal Cylinder Heater from Below," *Journal of Applied Mathematics and Mechanics*, Vol. 25, No. 6, 1961, pp. 1551–1558.